High-affinity DNA-targeting using Readily Accessible Mimics of N2'-Functionalized 2'-Amino-α-L-LNA

Saswata Karmakar,[†] Brooke A. Anderson,[†,§] Rie L. Rathje,[†,‡,§] Sanne Andersen,[†,‡, §] Troels B. Jensen,[‡] Poul Nielsen[‡] and Patrick J. Hrdlicka[*,†]

[†]Department of Chemistry, University of Idaho, Moscow, ID-83844-2343, USA

[§]Nucleic Acid Center, Institute for Physics and Chemistry, University of Southern Denmark, 5230 Odense M, Denmark

Contents

Additional discussion regarding formation of cyclic N2',O3'-hemiaminal ether. The structure of the cyclic N2',O3'-hemiaminal ether byproduct (Scheme S1) is supported by the following ^{1}H NMR observations (500 MHz, DMSO-d_6, results not shown): a) appearance of the hemiaminal ether proton as a singlet at 6.07 ppm; b) absence of an exchangeable signal corresponding to a 3'-OH group, c) absence of a signal corresponding to a CH_2-group linking the O2'-position and the pyrene moiety, and, d) appearance of the H1'-signal as a singlet at 6.13 ppm indicating formation of a restricted *North* type furanose conformation unlike what is observed for **6Q** (H1' signal appearing as a doublet at 6.43 ppm, J = 8.2 Hz). Despite formation of a new stereocenter, we only observed one set of signals, suggesting that only one of the diastereomers of the cyclic N2',O3'-hemiaminal ether byproduct is formed.

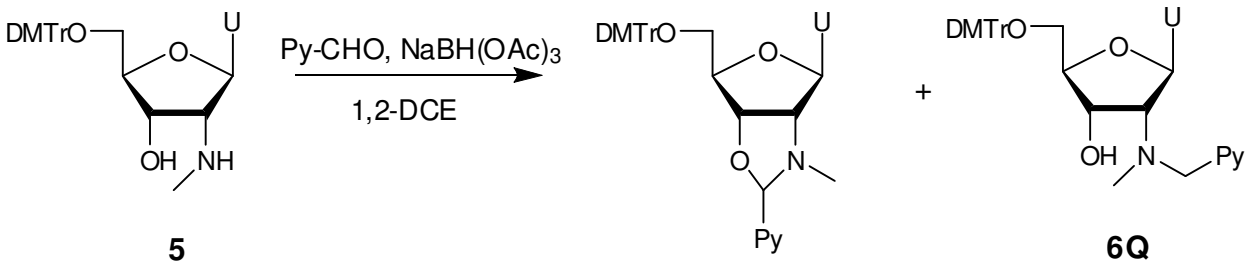

5 **6Q**

Scheme S1. Formation of cyclic N2',O3'-hemiaminal ether during **5→6Q**

Table S1. Representative RP-HPLC protocol.[a]

t [min]	Buffer A [v%]	Buffer B [v%]
0	100	0
2	100	0
50	30	70
64	0	100
69	0	100

[a] Buffer A is 0.05 M TEAA (triethyl ammonium acetate) pH 7.0 while buffer B is 75% MeCN in H_2O v/v. A flow rate of 1.2 mL/min was used.

Table S2. MALDI-MS of ONs modified with O2'-alkylated RNA monomers.[a]

ONs	Sequence	Calc. *m*/*z* [M]	Found *m*/*z* [M+H]
W1	5'-G**W**G ATA TGC	2880	2881
W2	5'-GTG A**W**A TGC	2880	2881
W3	5'-GTG ATA **W**GC	2880	2881
W4	3'-CAC **W**AT ACG	2809	2810
W5	3'-CAC TA**W** ACG	2809	2810
X1	5'-G**X**G ATA TGC	2954	2955
X2	5'-GTG A**X**A TGC	2954	2955
X3	5'-GTG ATA **X**GC	2954	2955
X4	3'-CAC **X**AT ACG	2883	2884
X5	3'-CAC TA**X** ACG	2883	2884
X6	3'-CAC **X**A**X** ACG	3085	3086
X7	5'-G**X**G A**X**A **X**GC	3358	3359
Y1	5'-G**Y**G ATA TGC	2968	2969
Y2	5'-GTG A**Y**A TGC	2968	2969
Y3	5'-GTG ATA **Y**GC	2968	2969
Y4	3'-CAC **Y**AT ACG	2897	2898
Y5	3'-CAC TA**Y** ACG	2897	2898
Y6	3'-CAC **Y**A**Y** ACG	3113	3114
Y7	5'-G**Y**G A**Y**A **Y**GC	3400	3401
Z1	5'-G**Z**G ATA TGC	3066	3067
Z2	5'-GTG A**Z**A TGC	3066	3067
Z3	5'-GTG ATA **Z**GC	3066	3067
Z4	3'-CAC **Z**AT ACG	2995	2996
Z5	3'-CAC TA**Z** ACG	2995	2996
Z6	3'-CAC **Z**A**Z** ACG	3309	3310
Z7	5'-G**Z**G A**Z**A **Z**GC	3694	3695

[a] For structure of monomers **V**-**Z** see Figure 1 in the main manuscript.

Table S3. MALDI-MS of ONs modified with N2'-functionalized 2'-amino-2'-deoxy-2'-*N*-methyl-uridine monomers.[a]

ONs	Sequence	Calc. *m*/*z* [M]	Found *m*/*z* [M+H]
Q1	5'-G**Q**G ATA TGC	2982	2983
Q2	5'-GTG A**Q**A TGC	2982	2983
Q4	3'-CAC **Q**AT ACG	2911	2912
Q5	3'-CAC TA**Q** ACG	2911	2912
Q6	3'-CAC **Q**A**Q** ACG	3140	3141
S1	5'-G**S**G ATA TGC	2996	2997
S2	5'-GTG A**S**A TGC	2996	2997
S4	3'-CAC **S**AT ACG	2925	2926
S5	3'-CAC TA**S** ACG	2925	2926
S6	3'-CAC **S**A**S** ACG	3168	3169
V1	5'-G**V**G ATA TGC	3009	3010
V2	5'-GTG A**V**A TGC	3009	3010
V4	3'-CAC **V**AT ACG	2938	2939
V5	3'-CAC TA**V** ACG	2938	2939
V6	3'-CAC **V**A**V**ACG	3195	3196

[a] For structure of monomers **V**-**Z** see Figure 1 in the main manuscript.

Representative thermal denaturation curves.

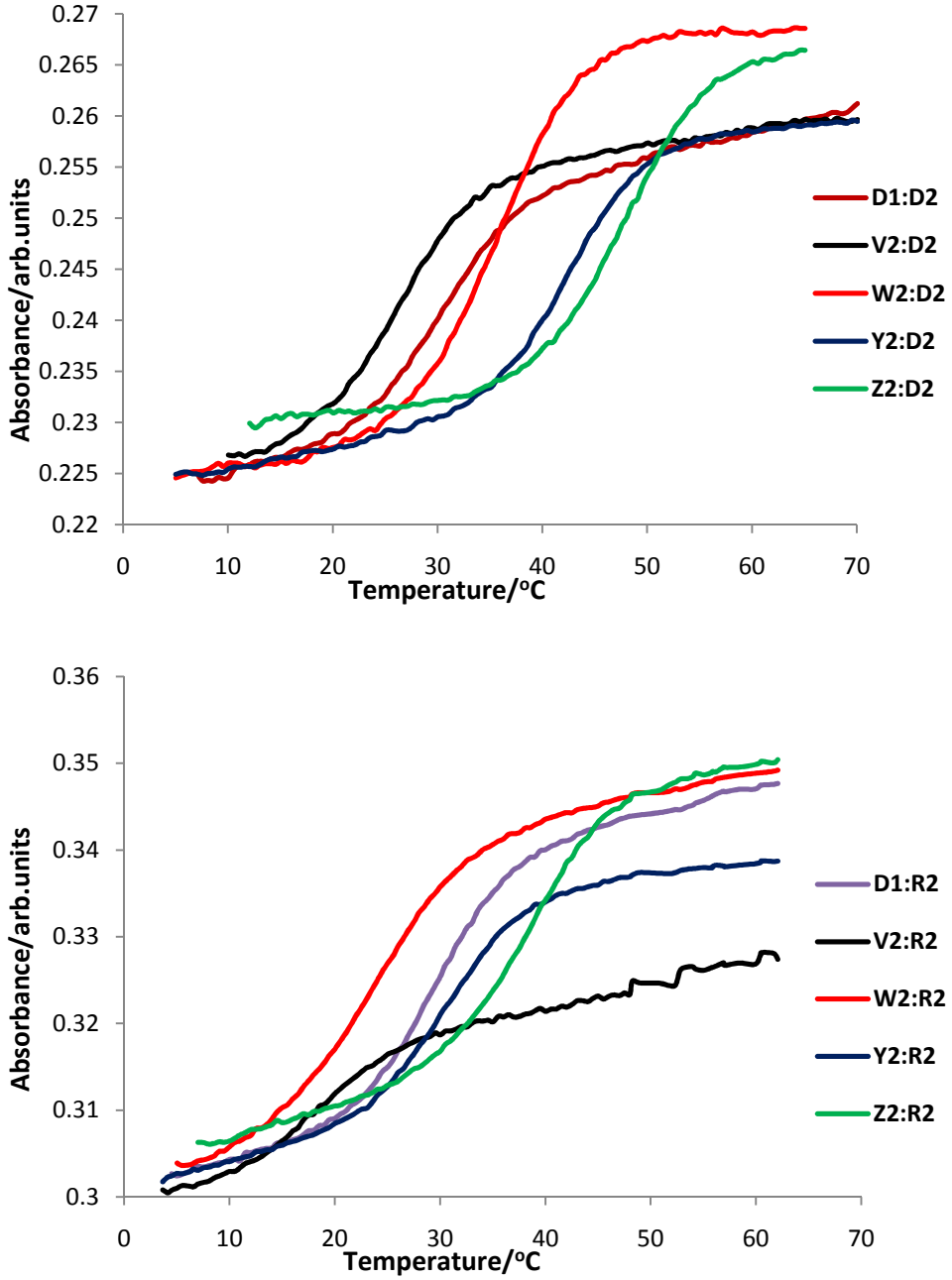

Figure S1. Thermal denaturation curves of duplexes between **V2-Z2** and complementary DNA (upper panel) or RNA (lower panel) targets. Unmodified reference duplexes are denoted **D1:D2** and **D1:R2**.

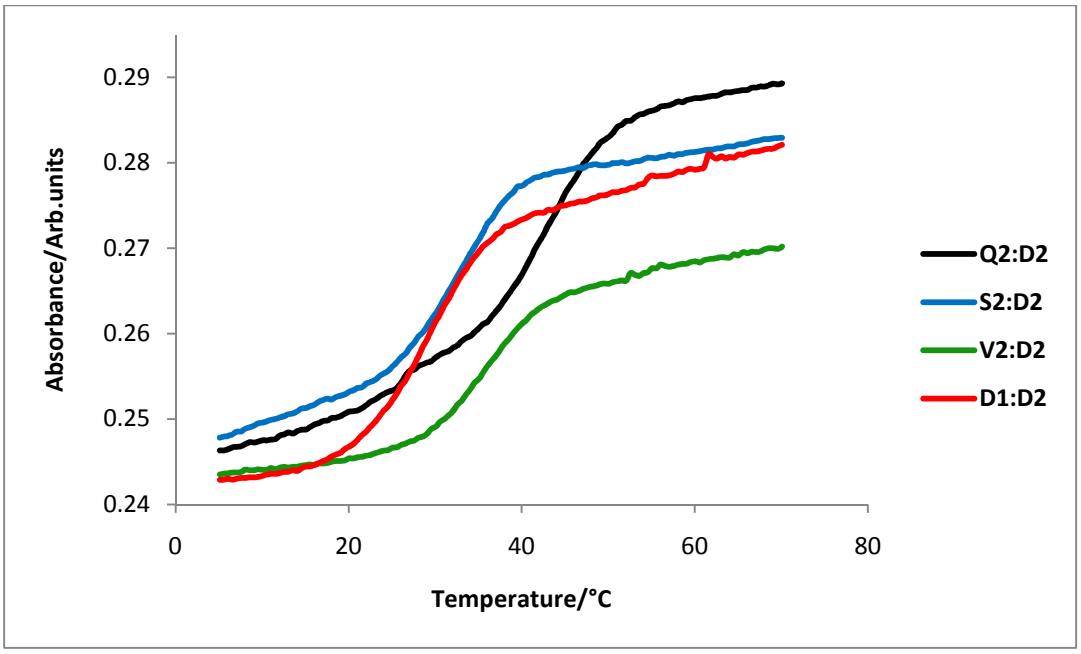

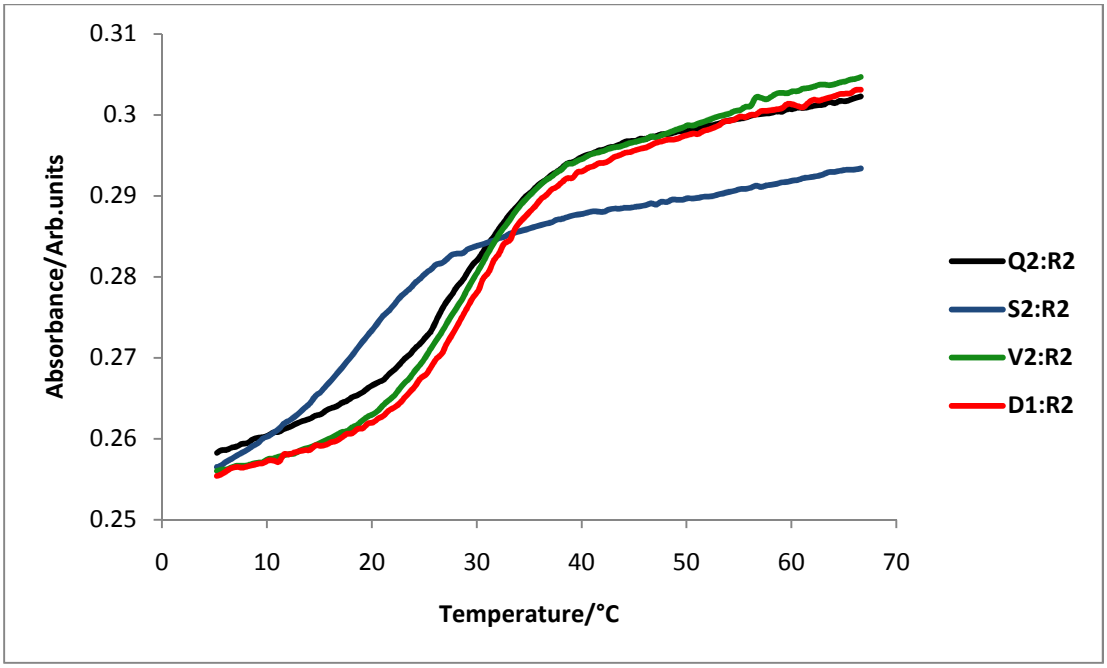

Figure S2. Thermal denaturation curves of duplexes between **Q2-V2** and complementary DNA (upper panel) or RNA (lower panel) targets. Unmodified reference duplexes are denoted **D1:D2** and **D1:R2**.

Table S4. Discrimination of mismatched RNA targets by **B2**-series and reference strands.[a]

			RNA: 3′-CAC U**B**U ACG			
			T_m [°C]	ΔT_m[°C]		
ON	**Sequence**	**B** =	A	C	G	U
D1	5′-GTG ATA TGC		**26.5**	<–16.5	–4.5	<–16.5
W2	5′-GTG A**W**A TGC		**16.0**	–1.0	+0.5	+6.0
X2	5′-GTG A**X**A TGC		**22.5**	–11.5	–5.0	<–12.5
Y2	5′-GTG A**Y**A TGC		**31.0**	–17.5	–3.5	-9.5
Z2	5′-GTG A**Z**A TGC		**37.0**	–12.0	-9.0	-13.0
Q2	5′-GTG A**Q**A TGC		**29.0**	–16.5	–0.5	–13.0
S2	5′-GTG A**S**A TGC		**18.0**	<–8.5	–6.0	–6.0
V2	5′-GTG A**V**A TGC		**28.0**	–16.5	–1.0	–7.5
L2[S1]	5′-GTG A**L**A TGC		**31.5**	–12.0	–1.0	-4.5

[a]For conditions of thermal denaturation experiments, see Table 1. T_m-values of fully matched duplexes are shown in bold. ΔT_m = change in T_m relative to fully matched DNA:RNA duplex.

Discussion of RNA mismatch data. Reference strand **D1** displays the expected specificity profile against mismatched RNA targets, i.e., a) formation of mismatched duplexes with reduced thermostability, and b) less efficient discrimination of targets leading to formation of U:rG-mismatched base pairs (Table S4). Monomers **Q**-**Z** fall into very distinctive categories with respect to RNA target affinity/specificity (Fig. S3), i.e., O2'-Nap monomer **W** (very poor/very poor); N2'-PyCO monomer **S** (very poor/poor); O2'-Py monomer **X** (very poor/moderate); N2'-PyAc monomer **V** (poor/poor); N2'-PyMe monomer **Q** (poor/poor); O2'-PyMe monomer **Y** (moderate/poor); regular DNA (moderate/moderate); O2'-CorMe monomer **Y** (high/moderate) and N2'-PyMe-α-L-LNA monomer **L** (high/very poor).

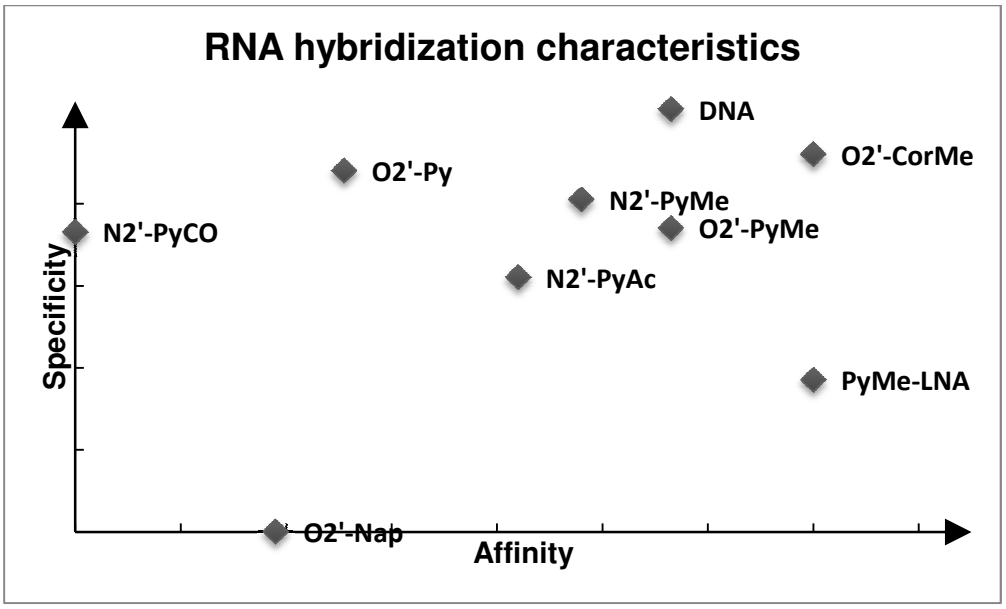

Figure S3. Representation of RNA hybridization characteristics (affinity vs specificity) of ONs modified with monomers **Q**-**Z** relative to unmodified DNA strand.

Absorption data for modified ONs.

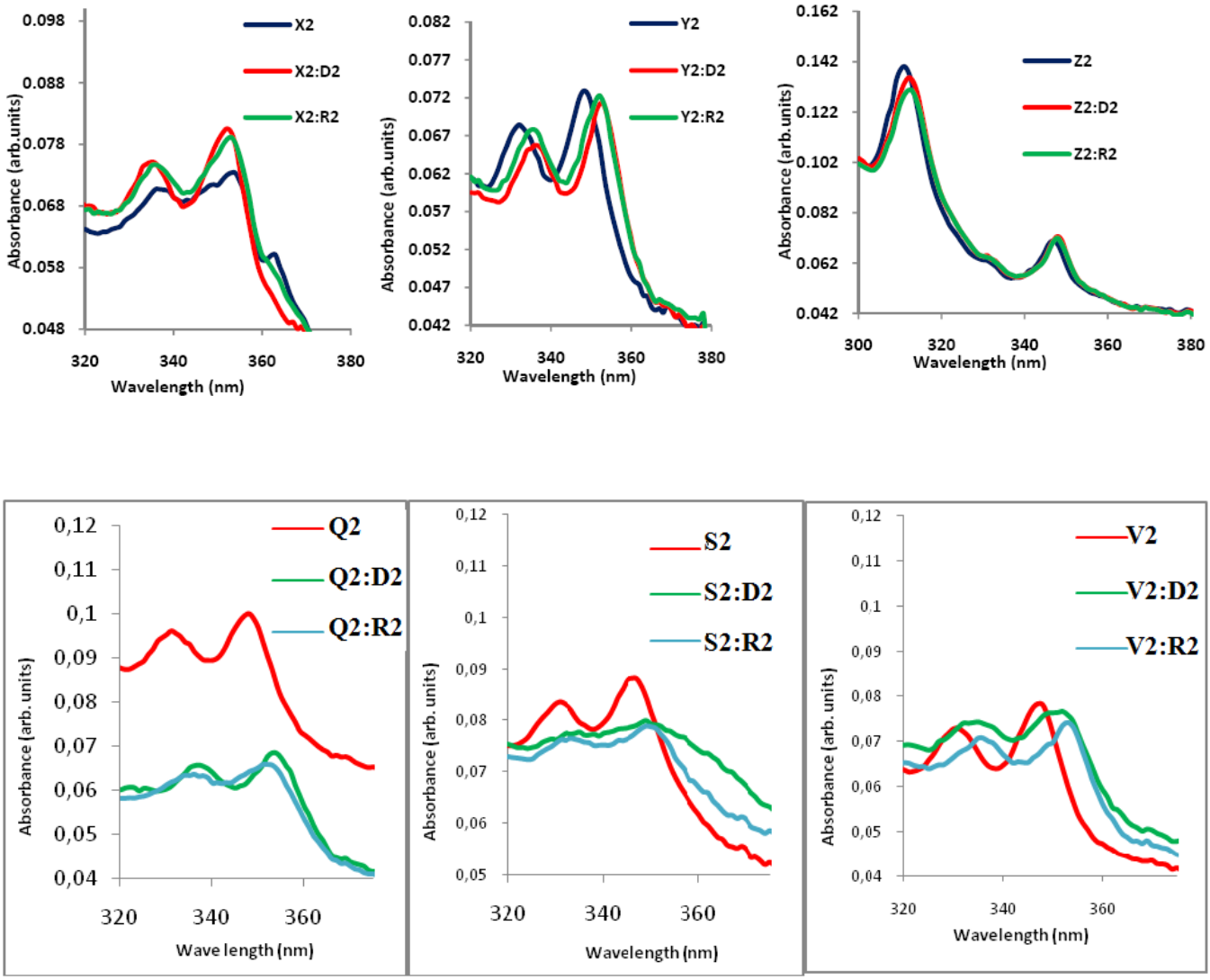

Figure S4. Absorption spectra of **X2**, **Y2, Z2, Q2, S2** and **V2** and their duplexes with complementary DNA (**D2**) and RNA (**R2**) targets. For experimental conditions see Table S5.

Table S5. Absorption maxima in the 320-360 nm region for ONs modified with O2'-alkylated RNA monomers **X**-**Z** or 2'-*N*-(pyren-1-yl)methyl-2'-amino-α-L-LNA monomer **L** in the presence or absence of complementary DNA/RNA targets.[a]

			$\lambda_{max}[\Delta\lambda_{max}]$ (nm)											
		B=	**X**			**Y**			**Z**			**L**^{S1}		
ON	Sequence		ss	+DNA	+RNA	ss	+DNA	+RNA	ss	+DNA	+RNA	ss	+DNA	+RNA
B1	5'-G**B**G ATA TGC		349	352[+3]	351[+2]	350	353[+3]	352[+2]	347	348[+1]	348[+1]	348	350[+2]	*349[+1]*
B2	5'-GTG A**B**A TGC		353	352[-1]	352[±0]	348	353[+5]	352[+4]	347	348[+1]	348[+1]	347	351[+4]	349[+2]
B3	5'-GTG ATA **B**GC		352	352[±0]	*352[±0]*	350	353[+3]	352[+2]	348	348[±0]	348[±0]	348	351[+3]	*350[+2]*
B4	3'-CAC **B**AT ACG		350	352[+2]	*352[+2]*	350	352[+2]	352[+2]	347	348[+1]	348[+1]	348	350[+2]	*348[±0]*
B5	3'-CAC TA**B** ACG		353	352[-1]	352[-1]	349	353[+4]	352[+3]	347	348[+1]	347[±0]	348	350[+2]	349[+1]

[a] Measurements were performed at room temperature (monomer **L**), 10 °C (monomer **Z**) and 7 °C (monomer **X** and **Y**) using a spectrophotometer and quartz optical cells with a 1.0 cm path length. Buffer conditions are as for thermal denaturation experiments. Values in italics are for duplexes with low thermostability (partial duplex dissociation at experimental temperature possible).

Table S6. Absorption maxima in the 320-360 nm region for ONs modified with N2'-functionalized 2'-*N*-methyl 2'-aminodeoxyuridine monomers **Q/S/V** in the presence or absence of complementary DNA/RNA targets.[a]

			$\lambda_{max}[\Delta\lambda_{max}]$ (nm)											
		B=	**Q**			**S**			**V**			**L**^{S1}		
ON	Sequence		ss	+DNA	+RNA	ss	+DNA	+RNA	ss	+DNA	+RNA	ss	+DNA	+RNA
B1	5'-G**B**G ATA TGC		349	353[+4]	351[+2]	347	351[+4]	*348[+1]*	348	352[+4]	352[+4]	348	350[+2]	*349[+1]*
B2	5'-GTG A**B**A TGC		348	353[+5]	351[+3]	346	349[+3]	349[+3]	347	352[+5]	353[+6]	347	351[+4]	349[+2]
B4	3'-CAC **B**AT ACG		349	354[+5]	349[±0]	348	350[+2]	*348[±0]*	349	353[+4]	352[+3]	348	350[+2]	*348[±0]*
B5	3'-CAC TA**B** ACG		348	354[+6]	352[+4]	346	348[+2]	350[+4]	347	352[+5]	352[+5]	348	350[+2]	349[+1]

[a] Measurements were performed at 5 °C. See Table S5 for further information on experimental conditions.

Steady-state fluorescence emission spectra for modified ONs.

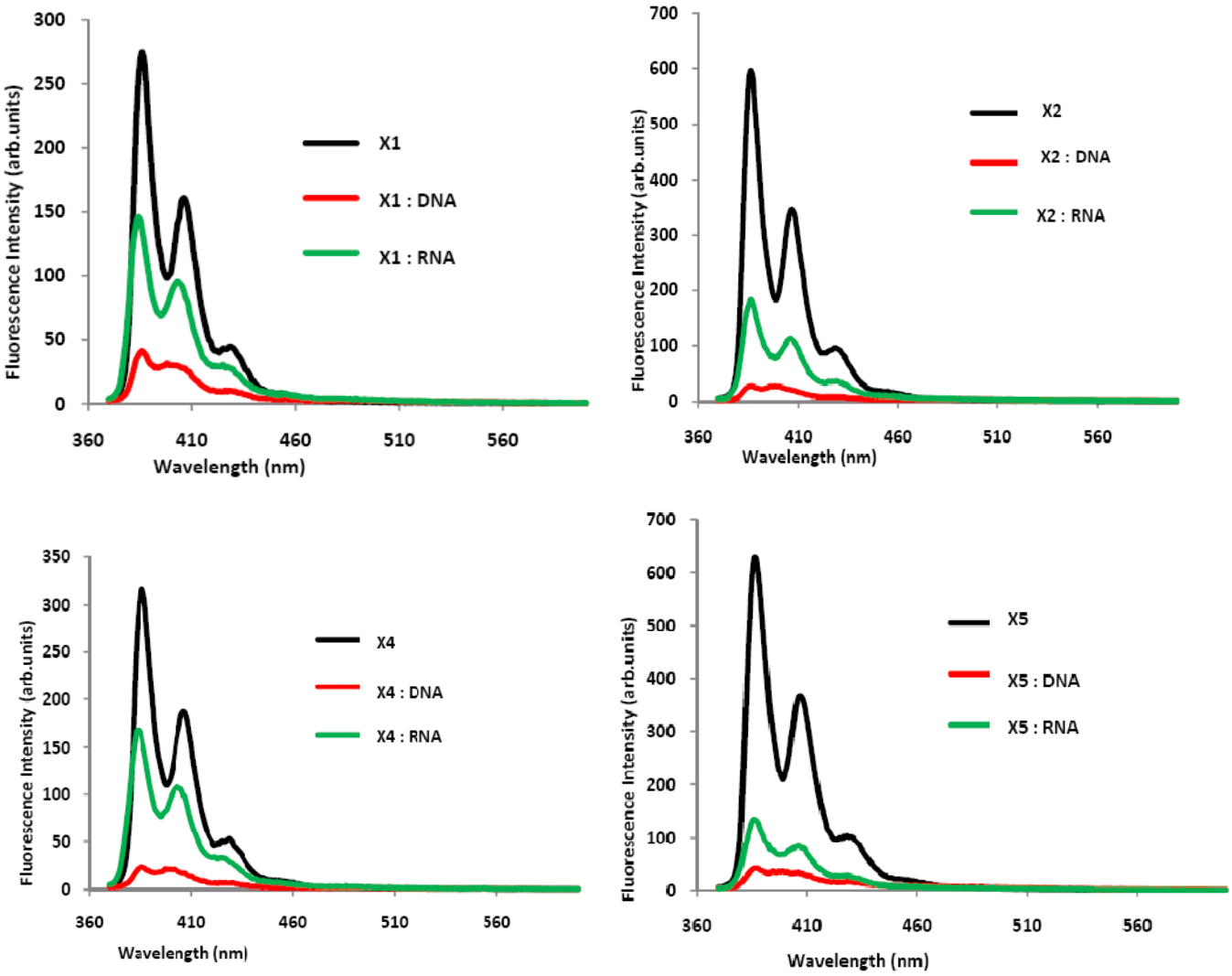

Figure S5. Fluorescence emission spectra of **X**-series in presence or absence of complementary DNA/RNA (λ_{ex} = 350 nm; T = 5 °C; [ON] = 1.0 μM). Please note that different Y-axes are used.

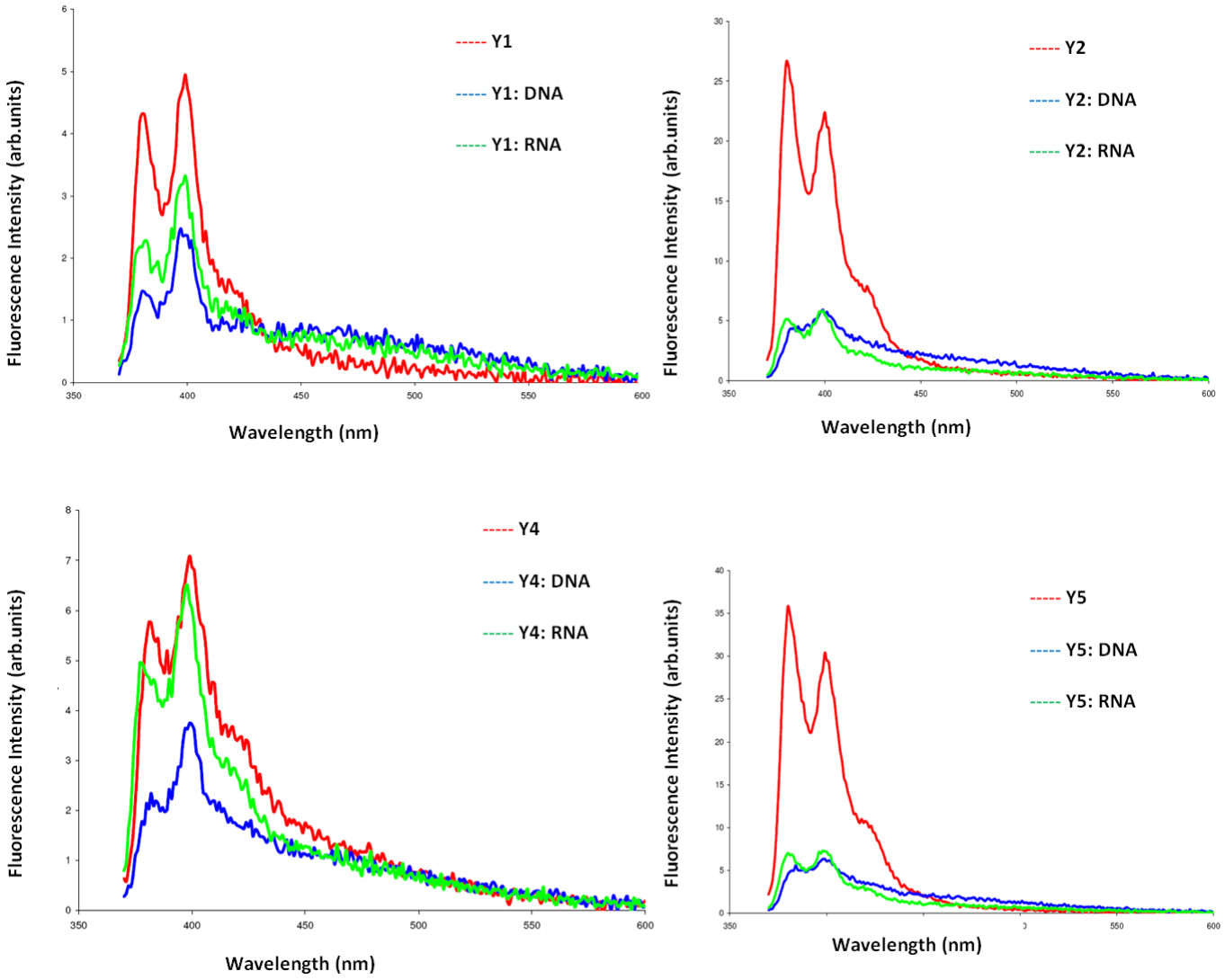

Figure S6. Fluorescence emission spectra of **Y**-series in presence or absence of complementary DNA/RNA (λ_{ex} = 350 nm; T = 5 °C; [ON] = 1.0 µM). Please note that different Y-axes are used.

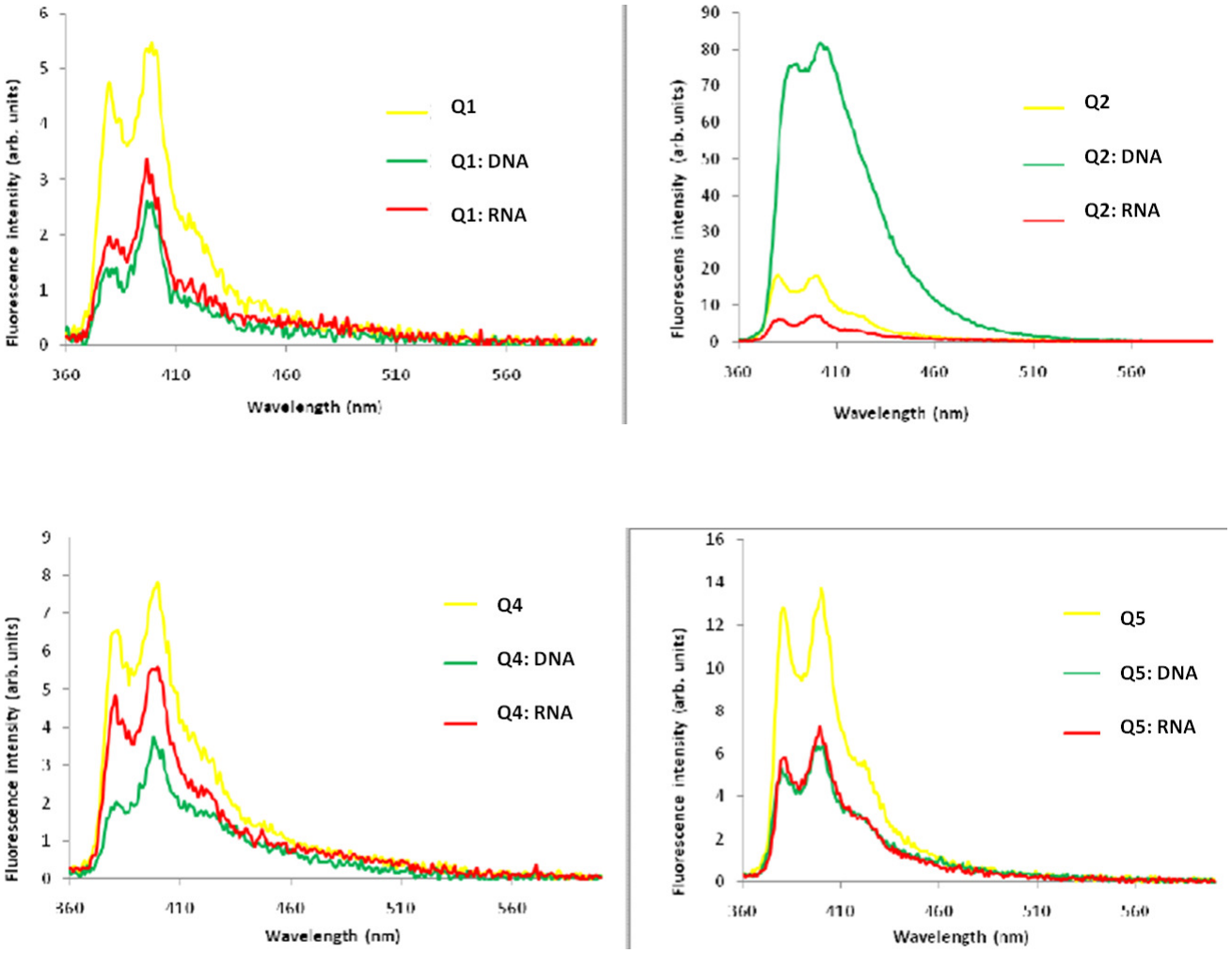

Figure S7. Fluorescence emission spectra of **Q**-series in presence or absence of complementary DNA/RNA (λ_{ex} = 350 nm; T = 5 °C; [ON] = 1.0 μM). Please note that different Y-axes are used.

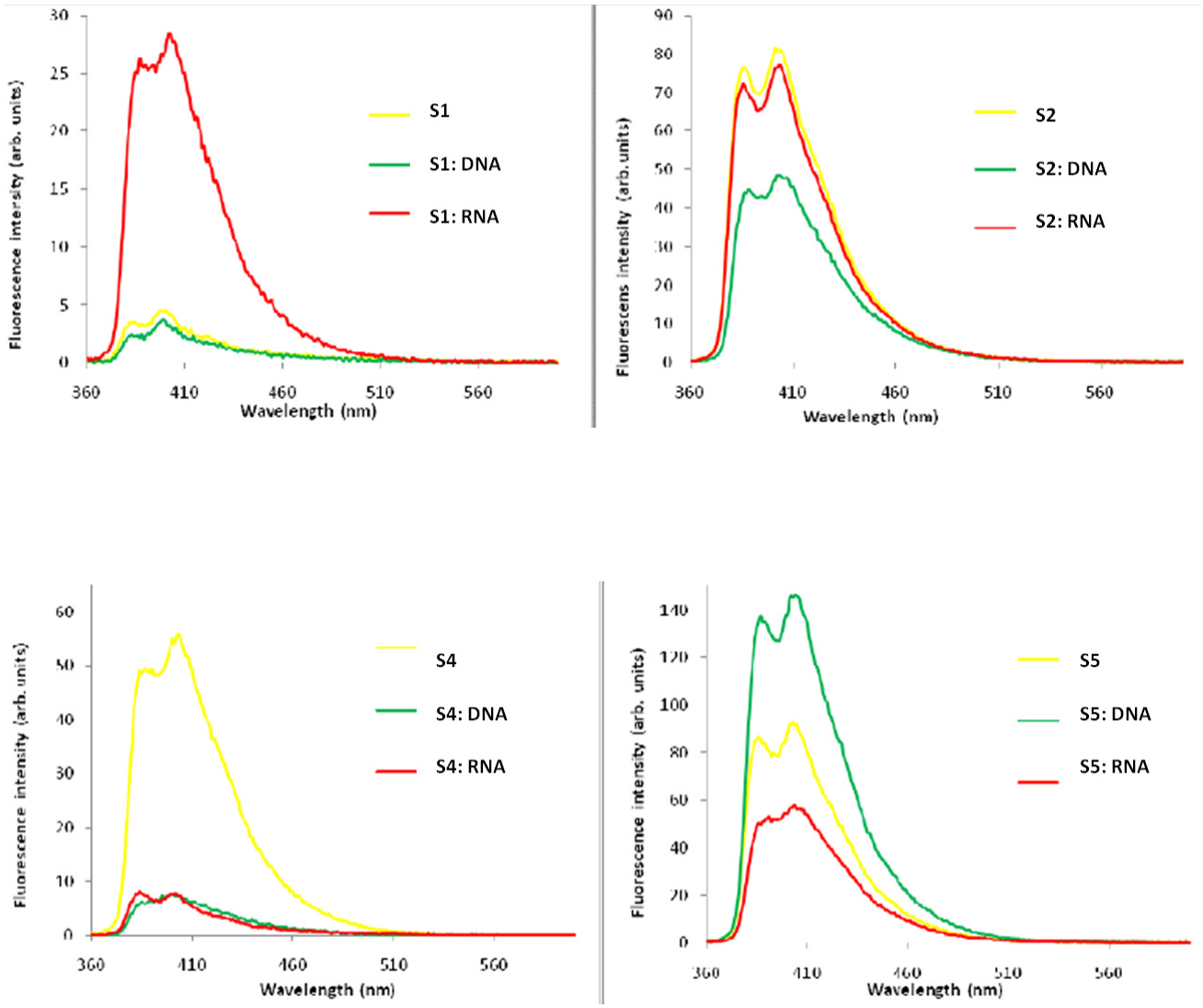

Figure S8. Fluorescence emission spectra of **S**-series in presence or absence of complementary DNA/RNA (λ_{ex} = 350 nm; T = 5 °C; [ON] = 1.0 μM). Please note that different Y-axes are used.

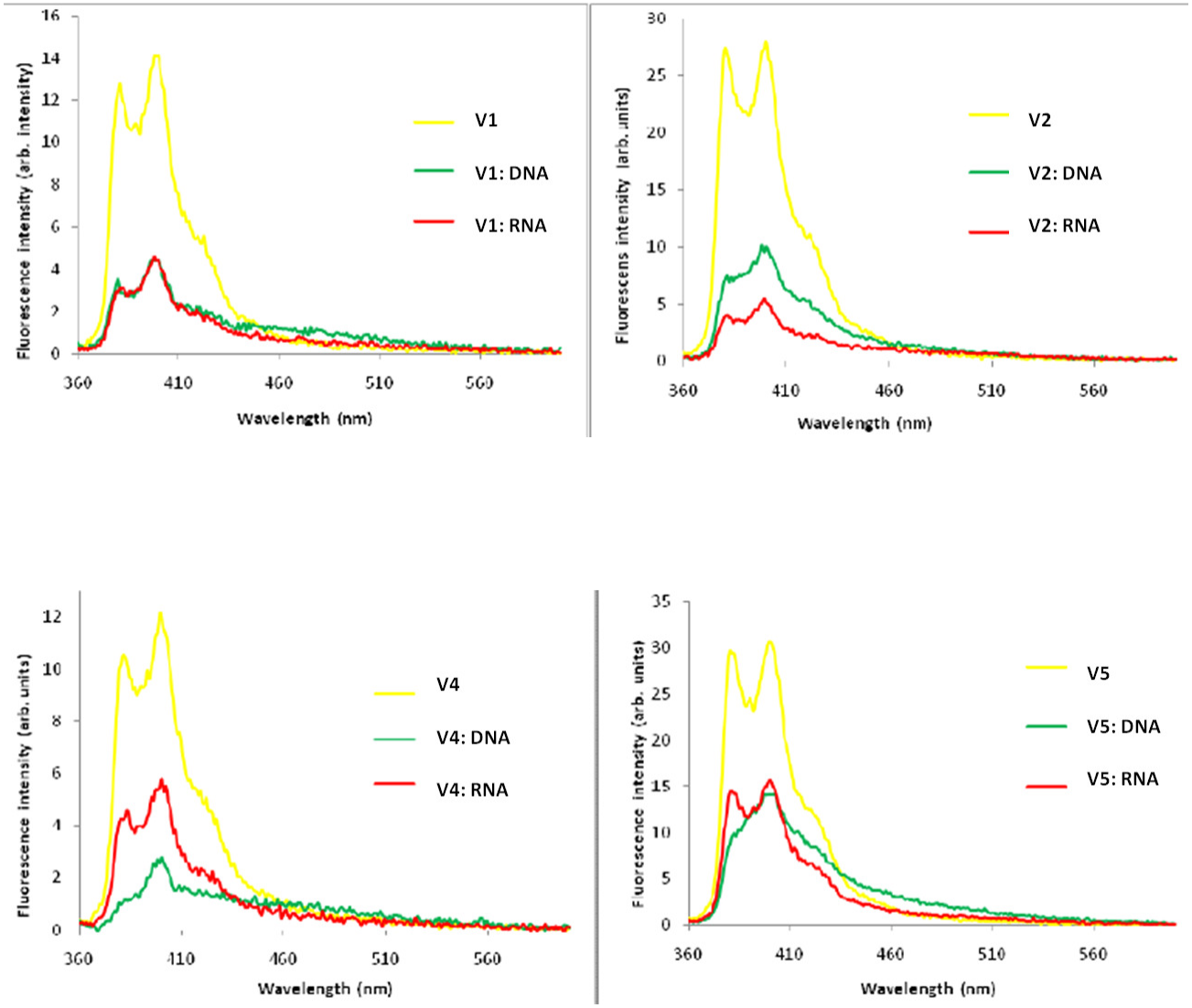

Figure S9. Fluorescence emission spectra of **V**-series in presence or absence of complementary DNA/RNA (λ_{ex} = 350 nm; T = 5 °C; [ON] = 1.0 μM). Please note that different Y-axes are used.

Additional discussion of fluorescence emission spectra. Fluorescence emission spectra involving O2'-Py-modified ONs (**X**-series) have several distinct features: (a) the emission profiles are sharper and considerably more intense than for the other pyrene-functionalized ONs and (b) low I_{III}/I_{I}-ratios are observed for single stranded probes and the corresponding duplexes with complementary RNA, while increased I_{III}/I_{I}-ratios are observed upon hybridization with complementary DNA (Figure S5). These observations suggest that the pyrene is positioned in a polar microenvironment in the single stranded state and in heteroduplexes with RNA, while positioned in a more hydrophobic region in duplexes with DNA,[S2] which is consistent with partial intercalation.

References.

(S1) Kumar, T. S.; Madsen, A. S.; Østergaard, M. E.; Sau, S. P.; Wengel, J.; Hrdlicka, P. J. *J. Org. Chem.* **2009**, *74*, 1070-1081.

(S2) Kalyanasundaram, K.; Thomas, J. K. *J. Am. Chem. Soc*. **1977**, *99*, 2039–2044.